

CHEMISTRY

AN ASIAN JOURNAL

www.chemasianj.org

Accepted Article

Title: POSS-phosphazene based porous material for adsorption of metal ions from water

Authors: Mikhail A. Soldatov and Hongzhi Liu

This manuscript has been accepted after peer review and appears as an Accepted Article online prior to editing, proofing, and formal publication of the final Version of Record (VoR). This work is currently citable by using the Digital Object Identifier (DOI) given below. The VoR will be published online in Early View as soon as possible and may be different to this Accepted Article as a result of editing. Readers should obtain the VoR from the journal website shown below when it is published to ensure accuracy of information. The authors are responsible for the content of this Accepted Article.

To be cited as: *Chem. Asian J.* 10.1002/asia.201901356

Link to VoR: <http://dx.doi.org/10.1002/asia.201901356>

A Journal of



A sister journal of *Angewandte Chemie*
and *Chemistry – A European Journal*

WILEY-VCH

POSS-phosphazene based porous material for adsorption of metal ions from water

Mikhail Soldatov, Hongzhi Liu*

Abstract: Development of adsorptive materials continues to be an important area of research for removal of heavy metal ions from waste water. The adsorption capacity can be modulated by both physical and chemical modification of the adsorbent. Herein, we combine the unique properties of polyhedral oligomeric silsesquioxane (POSS) and organocyclophosphazene as the building units to synthesize a hybrid porous material, abbreviated as PN-POSS. The synthetic method follows Heck reaction between hexa(4-bromophenoxy)cyclotriphosphazene and octavinylsilsesquioxane (OVS). The Brunauer–Emmett–Teller (BET) analysis shows that the material possesses micro- and meso pores of 1.5 and 3.8 nm size and surface area on the order of 500 m²/g. These attributes in combination with donor ability of the phosphazene units qualify the material for high adsorption of Pb²⁺, Hg²⁺ and Cu²⁺ ions with maximal adsorption capacities on the order of 1326, 1927 and 2654 mg/g, respectively. The adsorbent exhibits a good regeneration performance and can be effectively used for water treatment.

Introduction

Pollution with heavy metal ions is a serious ecological problem^[1]. When contaminated with water, these ions poses significant threat to environment and human health, they can accumulate in organisms for a long time period and cause cancer and other hard diseases^[2, 3]. At the present days there are several main approaches for water treatment and removal of heavy metal ions, such as ion exchange, adsorption, chemical deposition, membrane filtration and some their derivatives^[4]. The adsorption method is the most promising due to the technological simplicity, reusability and low cost. A good adsorbent needs to possess several properties like high adsorption capacity, chemical stability, good recycling properties etc. As a result, development of materials featuring intrinsic attributes such as stability, high surface area and tunable porosity has received considerable attention.

In the past, extensive studies have been reported to unravel the scope of such functional materials as activated porous carbon^[5], zeolites^[6], silica particles^[7-13], graphene oxide^[14, 15], metals or

metal oxides^[16, 17], natural minerals^[18-20] etc. as adsorbents for remediation of metal ions from water. The search for new and efficient adsorbents has prompted the design and synthesis of functional polymers^[21-27], metal organic frameworks^[28-30], polymeric composites^[31-33] and biohybrids^[34]. Nevertheless, the problem of low adsorption capacity of these materials still remains a challenge due to lack of synthetic methods which favor modulations in the physical properties and surface chemistry. It means that except high surface area the designed adsorbent should possess functional electron-rich groups on the surface, which will have strong interaction with metal ions. This high surface area can be achieved through the formation of porous structure. Polyhedral oligomeric silsesquioxanes (POSS) are well known for nanoscale dimension, rigidity, thermal stability due to strong siloxane bonds. As a result, they are being used actively as functional monomers for the creation of porous structures^[35]. Several methods including Heck^[36, 37] and Friedel-Crafts reactions^[38, 39] have been reported for the chemical transformation of POSS to hybrid porous materials.

Cyclic phosphazenes^[40] represent an interesting family of P-N bonded compounds and possess high thermal stability, fire-proofing and optical properties^[41]. Due to Lewis basicity of nitrogen atom, phosphazenes are known as a sequestering agents for metal ions^[42]. Phosphazene cyclomatrix polymers are highly cross-linked and can be obtained by nucleophilic substitution reaction of chlorocyclophosphazenes with phenols or amines^[43]. Practical applications of these materials as efficient adsorbents for dyes^[44], iodine^[45] or for CO₂ storage^[46-50] have been reported. Nevertheless, the use of phosphazene cyclomatrix materials for adsorption of metal ions has not been adequately addressed so far. Ozcan et al. have reported the synthesis of phosphazene microspheres by reacting hexachlorocyclotriphosphazene (HCCP) or octachlorocyclotetraphosphazene (OCCP) with diaminodiphenylmethane^[51] and demonstrated their use for removal of Pb²⁺ ions from water. Li et al. have reported the application of a porous phosphazene-based crosslinked polymer for effective extraction of uranium ions from water. The hybrid polymer was prepared by reacting HCCP with phenylenediamine, hydroquinone and phloroglucinol^[52, 53]. Mohanti et al. have used cyclotriphosphazene and trialkoxysilyl groups for the preparation of porous silica for adsorption of Cr₂O₇²⁻ ions, despite the relatively low surface area^[54-56].

In this study, we present the synthesis of a new hybrid material from the reaction of octavinylsilsesquioxane (OVS) with hexa(4-bromophenoxy)-cyclotriphosphazene using Pd(OAc)₂/(*o*-CH₃Ph)₃P as the catalyst. Adsorption property of the material for heavy metal ions is demonstrated and studied.

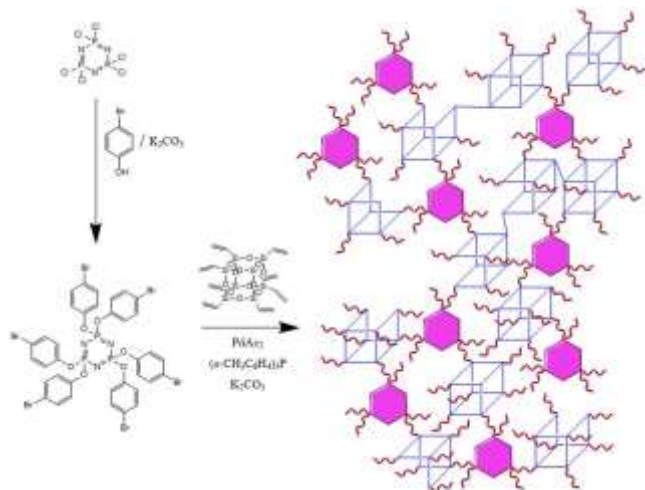
Dr. M. Soldatov, Prof. H. Liu
Key Laboratory of Special Functional Aggregated Materials, Ministry of Education, School of Chemistry and Chemical Engineering Shandong University
Jinan 250100, P. R. China.
E-mail: liuhongzhi@sdu.edu.cn

Supporting information for this article is given via a link at the end of the document

For internal use, please do not delete. Submitted_Manuscript

Results and Discussion

The phosphazene/POSS-based hybrid polymer (PN-POSS) is synthesized (**Scheme 1**) via Heck reaction of octavinylsilsesquioxane (OVS) with hexa(4-bromophenoxy)cyclotriphosphazene (HBPCP) in presence of Pd(OAc)₂/(*o*-CH₃Ph)₃P catalyst (see experimental section for details).



Scheme 1 Synthesis of PN-POSS by Heck reaction.

POSS units serve as rigid and nanosized building blocks, providing high porosity when phosphazene units serve as functional blocks, providing high adsorption capacity.

The FT-IR spectra of the polymer along with the precursors are shown in **Figure 1**. A comparative study allows to detect Si-O-Si (1100 cm⁻¹) and P-N (1200 cm⁻¹) segments arising from POSS and cyclo-phosphazene units, respectively in the polymer. The broadening of these peaks suggests the formation of cross-linked structure. The band at 3440 cm⁻¹ is attributed to Si-OH fragments due to partial cleavage of Si-O-Si bonds of the cage POSS during the Heck reaction^{57, 58}.

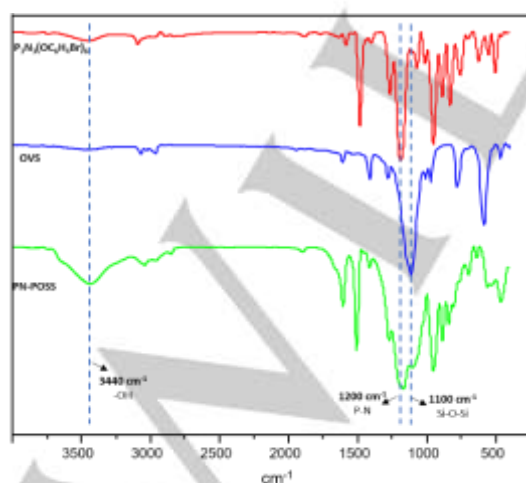


Figure 1 FTIR spectra of OVS, P₃N₃(OC₆H₄Br)₆ and PN-POSS.

In solid state ²⁹Si NMR spectrum (**Figure 2a**), the signals at -69.2 and -76.8 ppm are assigned to T₂ and T₃ units (T_n is C-Si(OSi)_n(OH)_{3-n}), and signals at -99.0 and -107.2 ppm suggest the formation of Q₃ and Q₄ units (Q_n is Si(OSi)_n(OH)_{4-n}) due to partial cleavage of the POSS cyclic structure (**Figure 2b**). Similar cleavage of siloxane bonds of POSS units due to presence of bases, such as triethylamine or NaHCO₃ during Heck reaction was reported previously^[36, 57, 58]. However, the relative intensity ratio T₃/(T+Q) is up to 0.57, which means that at least half cages in the network remain undamaged.

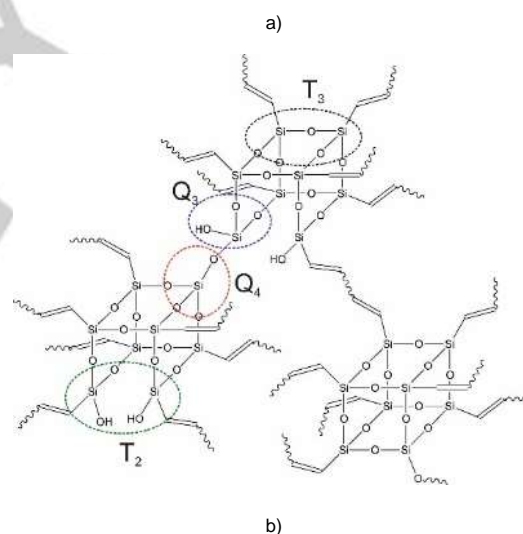
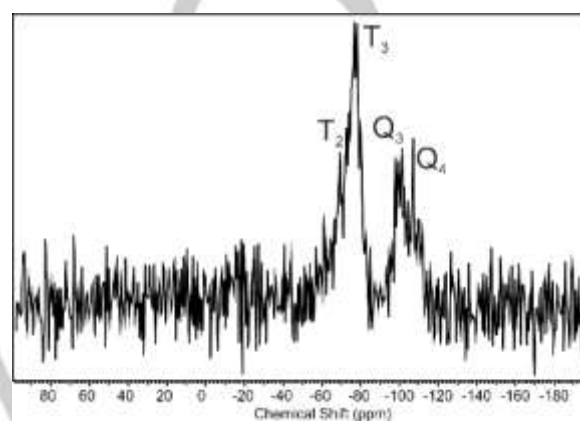


Figure 2 a) Solid ²⁹Si NMR MAS spectrum of PN-POSS; b) types of silicon atoms in porous material.

Solid state ¹³C NMR spectrum of PN-POSS (**Figure 3a**) reveals multiple peaks at 121.3, 127.6, 135.1 and 151.3 ppm and are assigned to ethylene and phenylene units. Peak at 50 ppm is assigned to residual methanol after extraction process. Solid state ³¹P NMR spectrum exhibits a distinct signal 8.5 ppm (**Figure 3b**) and confirms the retention of cyclotriphosphazene structure and no reactions on phosphazene rings, such as ring-opening or resubstitution, take place.

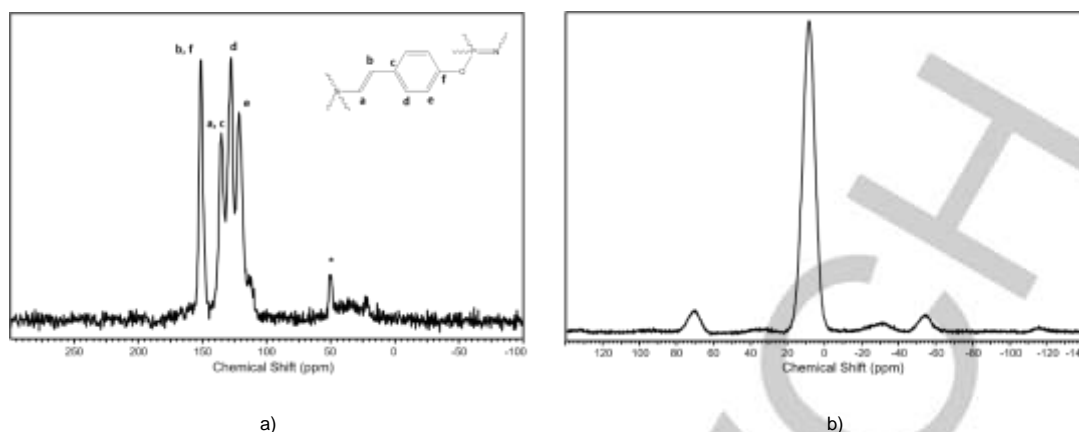


Figure 3 Solid ^{13}C (a) and ^{31}P (b) CP/MAS NMR spectra of PN-POSS.

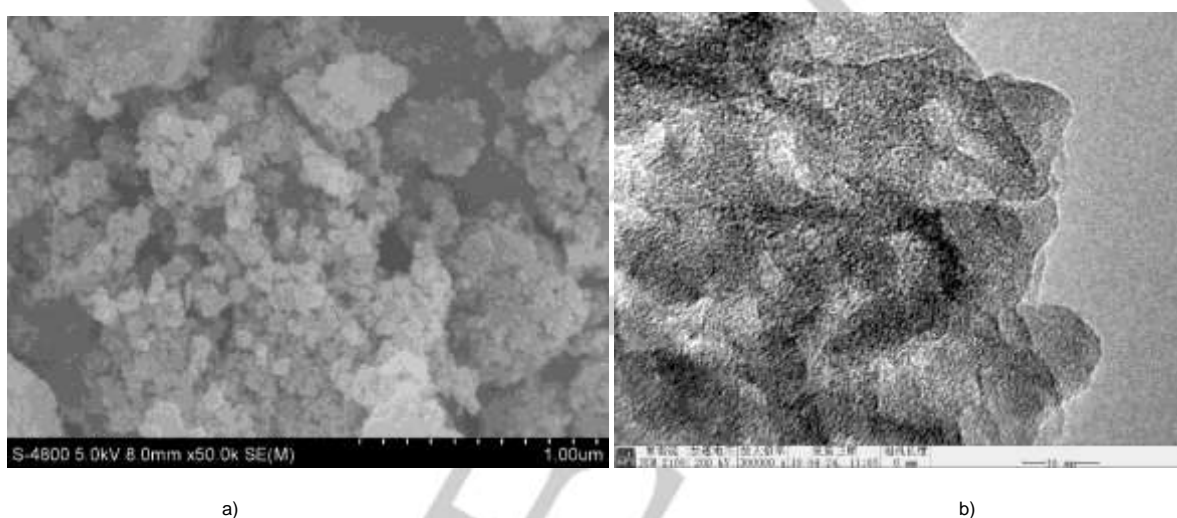


Figure 4 SEM (a) and TEM (b) of PN-POSS.

Powder X ray diffraction profile (**Figure S2**) exhibits the amorphous structure of porous polymer. As evident from SEM micrograph, morphology of the polymer features aggregated particles with size of about 100 nm (**Figure 4a**). TEM image shows that the material exhibits the amorphous structure with homogeneously distributed pores (**Figure 4b**).

The porous property is measured by nitrogen adsorption at 77 K (**Figure 5**). Adsorption/desorption curve can be defined as type IV isotherm according to IUPAC manual. The material shows sharp uptake at relatively low pressure, which subsequently increases gradually at higher pressure. A clear hysteresis loop indicates the presence of mesoporous content. Non-closed character of the hysteresis loop is usually regarded as the occurrence of swelling polymer because of the relative flexibility linkage between cage and phosphazene ring ^[59]. Surface area, calculated by BET equation, is 500 m^2/g and micropore surface area, calculated by t-plot method, is 152 m^2/g . The total pore volume (V_{total}) of the PN-POSS is 0.39 cm^3/g and the ratio of the micropore volume to the total ($V_{\text{micro}}/V_{\text{total}}$) is 0.172 (17.2 %). Pore size distribution, calculated by nonlocal density functional theory (NL-DFT), has a clearly bimodal character with sizes of

pores of 1.5 and 3.8 nm. This might be ascribed to the steric hindrance of nanosized cubic OVS and its multifunctional feature. The similar isotherms and pore size distribution curves for POSS-based porous materials were found in previous works ^[60-62].

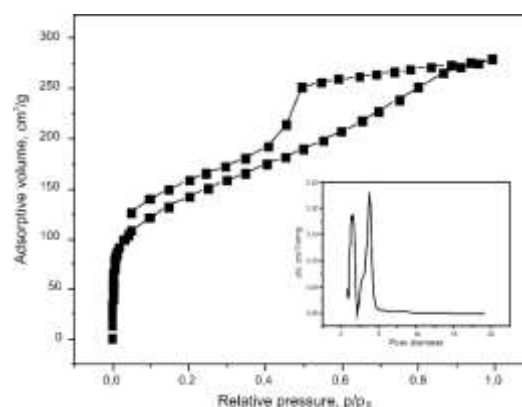


Figure 5 N_2 adsorption-desorption isotherm and pore size distribution PN-POSS.

For internal use, please do not delete. Submitted_Manuscript

Table 1 Summary of Langmuir and Freundlich model parameters for adsorption of metal ions by PN-POSS

Metal ion	Langmuir						Freundlich					
	Linear fitting			Nonlinear fitting			Linear fitting			Nonlinear fitting		
	q_m , mg/g	K_L , L/mg	R^2	q_m , mg/g	K_L , L/mg	R^2	K_F	n	R^2	K_F	n	R^2
Pb ²⁺	1326	0.0032	0.9679	1376	0.0030	0.9891	16.96	1.57	0.9936	15.48	1.60	0.9972
Hg ²⁺	1927	0.0012	0.9979	2113	0.0011	0.9987	4.97	1.23	0.9996	5.26	1.25	0.9997
Cu ²⁺	2654	0.0023	0.9989	2638	0.0023	0.9998	11.60	1.25	0.9964	17.79	1.34	0.9956

Thermogravimetry analysis (TGA) of the PN-POSS (**Figure S3**) shows that the polymer is stable up to 450 °C and subsequent wt loss occurs leaving a significant char yield (80 % wt) at 800 °C. An initial small weight loss at temperature less than 150 °C can be attributed to the evaporation of adsorbed water.

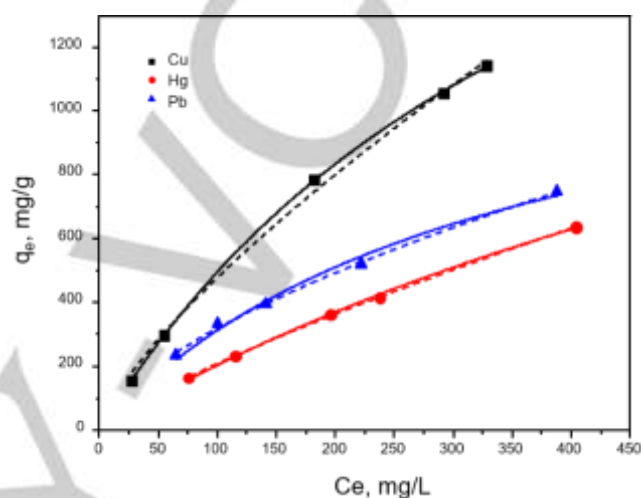
The adsorptive capacities were measured by adsorption isotherm experiments using solutions of metal ions in 50-500 mg/L concentration range (**Figure 6**). To study the adsorption properties, we used Langmuir and Freundlich models. Linear fitted forms of the models are as follows:

$$\frac{C_e}{q_e} = \frac{C_e}{q_m} + \frac{1}{K_L q_m} \quad (1)$$

$$\ln q_e = \ln K_F + \frac{1}{n} \ln C_e \quad (2)$$

where q_m is Langmuir maximum adsorption capacity (mg/g), K_L is Langmuir constant related to adsorption energy (L/mg), K_F is an indicator of adsorption capacity for Freundlich equation and n characterizes the adsorption intensity.

The plots obtained from these models are shown in **Figure S4** and the results are presented in **Table 1**. The correlation coefficients are higher in case of Freundlich adsorption. Nevertheless, correlation coefficients for Langmuir model are also appropriate in quite approximation. The results indicate that adsorption of ions has an intermediate position between monolayer and multilayer types with some predominance of the latter one. According to Langmuir approximation, maximum adsorption capacities for Pb²⁺, Hg²⁺ and Cu²⁺ are calculated as 1326, 1926 and 2654 mg/g, respectively. Such high adsorption capacities may be rationalized by the following factors. Positively charged metal ions can interact with electron-rich units of adsorbent. Nitrogen atoms in phosphazene fragments, due to strong Lewis bases properties, can serve as ligands and coordinate with metal ions to form stable complexes. Oxygen atoms in POSS and aryloxyphosphazene units can coordinate with metal ions as well. Another type of fragments is benzene rings, which can interact with metal ions through the conjugated π electron-rich aromatic system. The high porosity provides a large number of coordinating centers. Also, high content of polar silanol groups provides higher hydrophilicity and, as a result its better wetting by water solution.

**Figure 6** Adsorption isotherms for PN-POSS. Solid lines – Langmuir fitting, dashed lines – Freundlich fitting

For the deeper understanding of mechanism of adsorption, the sample with adsorbed Cu²⁺ ions was studied by FTIR (**Figure S5**) and XPS spectroscopy. In FTIR spectrum a peak in range of 680 cm⁻¹ is clearly shown which indicates formation of coordination bond Cu-N. In XPS Cu spectrum (**Figure 7a**) of sample after adsorption two characteristic peaks occurred at 934 and 953.6 eV, which are attributed to Cu 2p_{3/2} and Cu 2p_{1/2}, respectively. In XPS N 1s spectrum (**Figure 7b**) of the sample before adsorption one can see only one peak at 397.8 eV. After adsorption another peak appears at 399.8 eV (**Figure 7c**). This peak is attributed to nitrogen atoms, coordinated with metal ions. Due to this coordination the electron density on nitrogen atoms decreases and as a result binding energy shifts to higher values ($\Delta=2$ eV). O 1s and C 1s XPS spectra before and after adsorption remain the same, which indicates that metal ions interact mostly with nitrogen atoms of phosphazene ring and almost do not interact with other electron-rich units of the adsorbent.

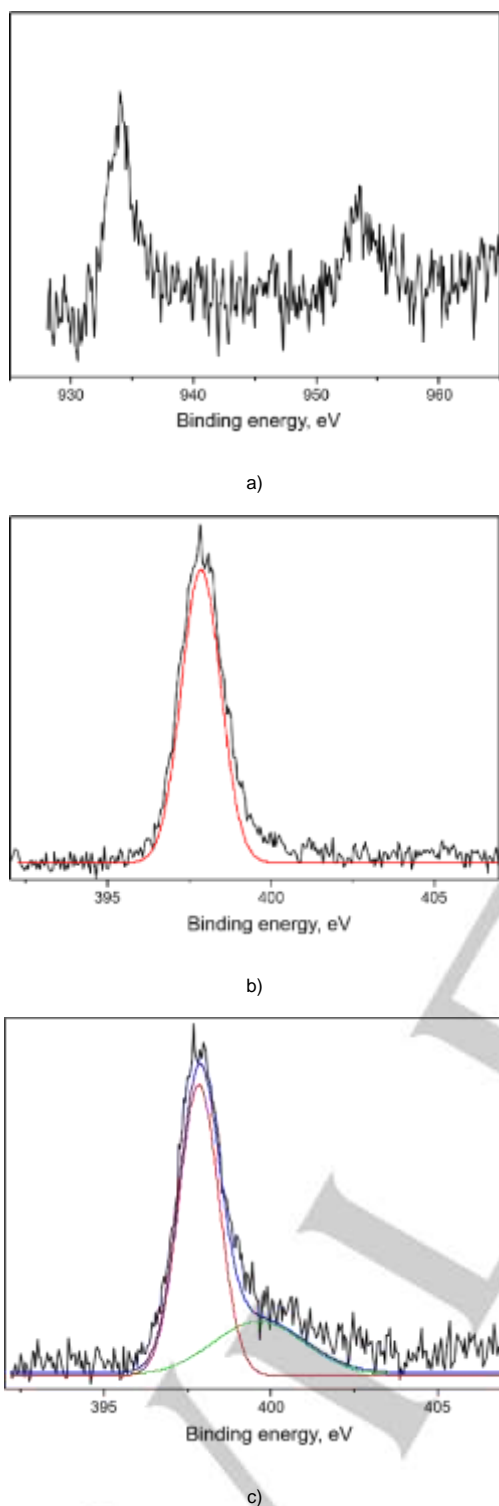


Figure 7 XPS spectra of PN-POSS after adsorption of Cu^{2+} . a) Cu 2p; b) N 1s before adsorption; c) N 1s after adsorption

To the best of our knowledge, the obtained material exhibits the highest values of adsorption capacities for these ions. In **Tables S1-S3** the adsorption properties for the other materials are shown. The adsorption capacities of phosphazene/POSS-based

adsorbent is higher than of adsorbents with higher surface area, which proves that chemical modification with the use of cyclophosphazene units could improve adsorption of heavy metal ions.

To check regeneration ability of the adsorbent, the solutions containing 5 mg/L of each metal ion (Pb^{2+} , Hg^{2+} , Cu^{2+}) separately in water were subjected to adsorption study using a dispersion of 20 mg of adsorbent. After first cycle, the removal of Cu^{2+} , Hg^{2+} and Pb^{2+} ions equal 80, 100 and 97 %, respectively (**Figure 8**). The adsorbent can be used after washing with 2M HCl, water, ethanol and dichloromethane and drying under vacuum for 12 h at 70 °C.

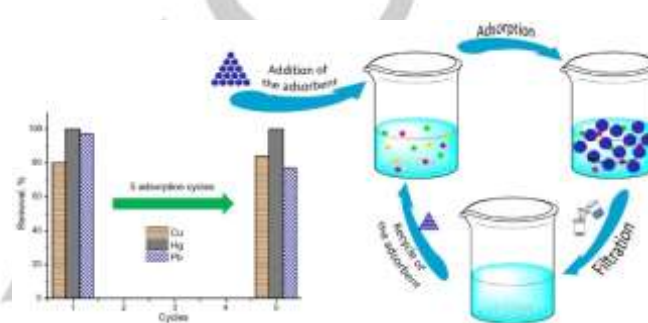


Figure 8 Regeneration performance of PN-POSS.

After five cycles the removals of Cu^{2+} and Hg^{2+} ions remain the same, although for Pb^{2+} ions the efficiency decreases to 77%. Decreasing of Pb^{2+} removal can be explained by following factors: from the adsorption data, it is evident that affinity of the adsorbent for Cu^{2+} and Hg^{2+} is much higher than for Pb^{2+} . Consequently, we believe that some active adsorption centers can be blocked by these competing cations during the adsorption/regeneration cycles which leads to decrease the adsorption of lead ions. In addition, different nature of the used metals allows to suggest that phosphazene/POSS-based adsorbents can be quite effective for the other heavy metal ions.

Conclusions

In conclusion, a novel porous hybrid polymeric material was synthesized by Heck reaction of octavinylsilsesquioxane (OVS) with hexakis(4-bromophenoxy)cyclotriphosphazene. The obtained polymer possesses micro- and mesoporous structure with surface area of 500 m^2/g and demonstrates outstanding adsorption towards such heavy metal ions as Cu^{2+} , Hg^{2+} and Pb^{2+} . Such high adsorption capacities are caused by synergetic combination of two factors: physical and chemical modification of adsorbent structure. The former is achieved by high surface area and porosity with the use of POSS as a rigid nano-sized building block, the latter by the use of cyclophosphazene units. The adsorbent exhibits good regeneration performance by simple filtration and washing. These results show that the obtained micro- and mesoporous adsorbent can be promising for waste water treatment. As this material possesses highly active coordinating nitrogen atoms, further investigations are

For internal use, please do not delete. Submitted_Manuscript

focused on the preparation of the metal-doped materials as heterogeneous catalysts with regeneration performance.

Experimental Section

THF was dried over Na/benzophenone and distilled before synthesis. DMF was dried over CaH₂ for 12 h at 80 °C and distilled under vacuum pressure. OVS was synthesized by following previous report^[63]. All the other chemicals were purchased from commercial suppliers and were used without further purification.

Synthesis of hexa(4-bromophenoxy)cyclotriphosphazene (HBPCP). 3.74 g (21.6 mmol) of 4-bromophenol and 4.5 g (32.61 mmol) of K₂CO₃ were dispersed in 30 mL THF and stirred in oil bath for 2h at 70 °C. To the mixture a solution of 0.94 g (2.7 mmol) hexachlorocyclotriphosphazene in 20 mL THF was added dropwise. Mixture was stirred under refluxing for 48 h. The solution was filtered and washed with brine. Organic layer was dried with MgSO₄ and solvent was rotary evaporated. The product was recrystallized from acetone and dried under vacuum at 50 °C for 5 h. Yield: 2.42 g (77 %). ³¹P NMR, CDCl₃: 8.73, s (Figure S1).

Synthesis of phosphazene/POSS-based hybrid porous material (PN-POSS). 0.19 g (0.3 mmol) of OVS, 0.56 g (0.48 mmol) of HBPCP, 0.027 g (0.12 mmol) of palladium diacetate, 0.11 g (0.36 mmol) of tri(*o*-tolyl)phosphine and 0.83 g (6 mmol) of K₂CO₃ were charged in oven-dried 3-necked flask with condenser and magnetic stirrer. Flask was vacuumed and filled with nitrogen. After that 10 mL of DMF were added and mixture was stirred for 20 min at room temperature. Then the mixture was stirred at 120 °C for 72 h. The solid polymer was filtered, washed with water, acetone and DCM. Then it was extracted with methanol (24 h) and DCM (24 h) and dried under vacuum at 70 °C for 24 h. PN-POSS was afforded as a black solid (0.58 g).

Acknowledgements

This research was supported by the National Natural Science Foundation of China (NSFC) (21574075, 21975144), Key Research and Development Program of Shandong province (2018GGX102034), Ministry of Science and Technology of the People's Republic of China (G20190015042, G20190015037) and Seed Fund Program for the International Research Cooperation of Shandong University.

Keywords: adsorption • heavy metal ions • hybrid porous materials • phosphazenes • POSS

- [1] S. Chowdhury, M. A. Jafar Mazumder, O. Al-Attas, T. Husain, *Sci. Total Environ.* **2016**, 569–570, 476–488.
- [2] P. K. Rai, S. S. Lee, M. Zhang, Y. F. Tsang, K.-H. Kim, *Environ. Int.* **2019**, 125, 365–385.
- [3] C. Li, K. Zhou, W. Qin, C. Tian, M. Qi, X. Yan, W. Han, *Soil Sediment. Contam. Int. J.* **2019**, 28, 380–394.
- [4] S. Bolisetty, M. Peydayesh, R. Mezzenga, *Chem. Soc. Rev.* **2019**, 48, 463–487.

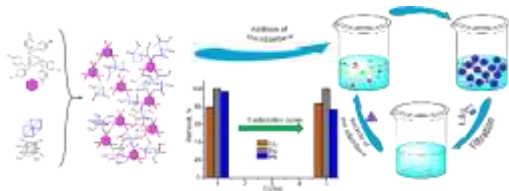
- [5] S.-A. Sajjadi, A. Meknati, E. C. Lima, G. L. Dotto, D. I. Mendoza-Castillo, I. Anastopoulos, F. Alakhras, E. I. Unuabonah, P. Singh, A. Hosseini-Bandegharae, *J. Environ. Manage.* **2019**, 236, 34–44.
- [6] A. A. Malhis, S. H. Arar, M. K. Fayyad, H. A. Hodali, *Ads. Sci. Tech.* **2018**, 36, 270–286.
- [7] S. Herrmann, L. De Matteis, J. M. de la Fuente, S. G. Mitchell, C. Streb, *Angew. Chem. Int. Ed.* **2017**, 56, 1667–1670.
- [8] S. Chatterjee, A. R. Paital, *Adv. Funct. Mater.* **2018**, 28, 1704726.
- [9] D. Kaliannan, S. Palaninaicker, V. Palanivel, M. A. Mahadeo, B. N. Ravindra, S. Jae-Jin, *Environ. Sci. Pollut. Res.* **2019**, 26, 5305–5314.
- [10] C.-W. Wu, Y. Yamauchi, T. Ohsuna, Kazuyuki Kuroda, *J. Mater. Chem.* **2006**, 16, 3091–3098
- [11] M. Nandi, J. Mondal, K. Sarkar, Y. Yamauchi, A. Bhaumik, *Chem. Commun.* **2011**, 47, 6677–6679
- [12] V. Malgras, J. Henzie, T. Takei, Y. Yamauchi, *Angew. Chem. Int. Ed.* **2018**, 57, 8881–8885
- [13] Y. Yamauchi, T. Nagaura, A. Ishikawa, T. Chikyow, S. Inoue, *J. Am. Chem. Soc.* **2008**, 130, 10165–10170
- [14] S. Ahmad, A. Ahmad, S. Khan, S. Ahmad, I. Khan, S. Zada, P. Fu, *J. Ind. Eng. Chem.* **2019**, 72, 117–124.
- [15] J. Zhang, X. Xie, C. Liang, W. Zhu, X. Meng, *J. Ind. Eng. Chem.* **2019**, 73, 233–240.
- [16] H. Ataee-Esfahani, J. Liu, M. Hu, N. Miyamoto, S. Tominaka, K. C. W. Wu, Y. Yamauchi, *Small* **2013**, 9, 1047–1051
- [17] B. P. Bastakoti, S. Ishihara, S.-Y. Leo, K. Ariga, K. C.-W. Wu, Y. Yamauchi, *Langmuir* **2014**, 30, 651–659
- [18] T. Wang, Y. Yang, J. Wang, J. Wu, L. Sun, Y. Du, Y. Li, H. Li, *RSC Adv.* **2019**, 9, 3816–3827.
- [19] C. Yan, L. Guo, D. Ren, P. Duan, *Mater. Letter.* **2019**, 239, 192–195.
- [20] Z. Shang, L. Zhang, X. Zhao, S. Liu, D. Li, *J. Environ. Manage.* **2019**, 231, 391–396.
- [21] W. Li, B. Ju, S. Zhang, *RSC Adv.* **2019**, 9, 6986–6994.
- [22] M. Mitra, M. Mahapatra, A. Dutta, J. S. D. Roy, M. Karmakar, M. Deb, H. Mondal, P. K. Chattopadhyay, A. Bandyopadhyay, N. R. Singha, *J. Hazard. Mater.* **2019**, 369, 746–762.
- [23] M. Mozaffari, M. R. S. Emami, E. Binaeian, *Int. J. Biol. Macromol.* **2019**, 123, 457–467.
- [24] M. I. Shariful, T. Sepehr, M. Mehrali, B. C. Ang, M. A. Amalina, *J. Appl. Polym. Sci.* **2018**, 45851.
- [25] W. Zhan, C. Xu, G. Qian, G. Huang, X. Tang, B. Lin, *RSC Adv.* **2018**, 8, 18723–18733.
- [26] N. R. Singha, M. Karmakar, M. Mahapatra, H. Mondal, A. Dutta, M. Deb, M. Mitra, C. Roy, P. K. Chattopadhyay, *J. Mater. Chem. A.* **2018**, 6, 8078–8100.
- [27] Y. O Al-Ghamdi, K. A Alamry, M. A Hussein, H. M Marwani, A. M Asiri, *Ads. Sci. Tech.* **2019**, 37, 139–159.
- [28] S. Jamshidifard, S. Koushkbaghi, S. Hosseini, S. Rezaei, A. Karamipour, A. Jafari rad, M. Irani, *J. Hazard. Mater.* **2019**, 368, 10–20.
- [29] L. Fu, S. Wang, G. Lin, L. Zhang, Q. Liu, J. Fang, C. Wei, G. Liu, *J. Hazard. Mater.* **2019**, 368, 42–51.
- [30] A. Nqombolo, A. Mpupa, A. S. Gugushe, R. M. Moutloali, P. N. Nomngongo, *Environ. Sci. Pollut. Res.* **2019**, 26, 3330–3339.
- [31] H. Fan, X. Ma, S. Zhou, J. Huang, Y. Liu, Y. Liu, *Carbohydr. Polym.* **2019**, 213, 39–49.
- [32] L. Xie, Z. Yu, S. M. Islam, K. Shi, Y. Cheng, M. Yuan, J. Zhao, G. Sun, H. Li, S. Ma, M. G. Kanatzidis, *Adv. Funct. Mater.* **2018**, 28, 1800502.
- [33] K. D. Nguyen, T. T. C. Trang, T. Kobayashi, *J. Appl. Polym. Sci.* **2019**, 47207.
- [34] Y. Zhang, K. Yan, F. Ji, L. Zhang, *Adv. Funct. Mater.* **2018**, 28, 1806340.
- [35] C. Zhang, F. Babonneau, C. Bonhomme, R. M. Laine, C. L. Soles, H. A. Hristov, A. F. Yee, *J. Am. Chem. Soc.* **1998**, 120, 8380–8391.
- [36] D. Wang, W. Yang, S. Feng, H. Liu, *Polym. Chem.* **2014**, 5, 3634–3642.
- [37] R. Sun, S. Feng, D. Wang, H. Liu, *Chem. Mater.* **2018**, 30, 6370–6376.

For internal use, please do not delete. Submitted_Manuscript

- [38] Y. Wu, D. Wang, L. Li, W. Yang, S. Feng, H. Liu, *J. Mater. Chem. A* **2014**, 2, 2160–2167.
- [39] D. Wang, E. Mejía, *ChemistrySelect* **2017**, 2, 3381–3387.
- [40] M. Gleria, R. De Jaeger, *Phosphazenes: a worldwide insight*. Nova Science Publishers Inc., New York, **2004**, p. 1047.
- [41] H. R. Allcock, *J. Inorg. Organomet. Polym. Mater.* **2006**, 16, 277–294.
- [42] V. Chandrasekhar, P. Thilagar, B. M. Pandian, *Coord. Chem. Rev.* **2007**, 251, 1045–1074.
- [43] C. Wan, X. Huang, *Mater. Today Commun.* **2007**, 11, 38–60.
- [44] J. Zhang, Z. Miao, J. Yan, X. Zhang, X. Li, Q. Zhang, Y. Yan, *Macromol. Rapid Commun.* **2018**, 1800730.
- [45] R. Muhammad, P. Mohanty, *J. Mol. Liq.* **2019**, 283 58–64
- [46] P. Rekha, U. Sahoo, P. Mohanty, *RSC Adv.* **2014**, 4, 34860–34863.
- [47] P. Mohanty, L. D. Kull, K. Landskron, *Nat. Commun.* **2011**, 2, 401
- [48] R. Muhammad, P. Rekha, P. Mohanty, *RSC Adv.* **2016**, 6, 17100–17105
- [49] R. Muhammad, P. Mohanty, *Langmuir* **2018**, 34, 2926–2932
- [50] R. Muhammad, M. Chaudhary, P. Mohanty, *J. CO₂ Util.* **2018**, 25, 302–309
- [51] T. A. Arici, S. M. Orum, Y. S. Demircioglu, A. Ozcan, A. S. Ozcan, *Phosphorus Sulfur Silicon Relat. Elem.* **2018**, 193, 721–730.
- [52] S. Zhang, X. Zhao, B. Li, C. Bai, Y. Li, L. Wang, R. Wen, M. Zhang, L. Ma, S. Li, *J. Hazard. Mater.* **2016**, 314, 95–104.
- [53] M. Zhang, Y. Li, C. Bai, X. Guo, J. Han, S. Hu, H. Jiang, W. Tan, S. Li, L. Ma, *ACS Appl. Mater. Interfaces.* **2018**, 10, 28936–28947.
- [54] P. Rekha, V. Sharma, P. Mohanty, *Microporous Mesoporous Mater.* **2016**, 219, 93–102.
- [55] P. Rekha, R. Muhammad, V. Sharma, M. Ramteke, P. Mohanty, *J. Mater. Chem. A.* **2016**, 4, 17866–17874.
- [56] P. Rekha, R. Muhammad and P. Mohanty, *RSC Adv.* **2015**, 5, 67690–67699.
- [57] M. Ge, H. Liu, *Chem. Eur. J.* **2018**, 24, 2224–2231.
- [58] M. Ge, H. Liu, *J. Mater. Chem. A.* **2016**, 4, 16714–16722.
- [59] Q. Chen, M. Luo, P. Hammershoj, D. Zhou, Y. Han, B. W. Laursen, C. G. Yan, B. H. Han, *J. Am. Chem. Soc.* **2012**, 134, 6084–6087.
- [60] D. Wang, W. Yang, S. Feng, H. Liu, *Polym. Chem.* **2014**, 5, 3634–3642.
- [61] D. Wang, W. Yang, S. Feng, H. Liu, *RSC Adv.* **2016**, 6, 13749–13756.
- [62] Y. Yan, R. M. Laine, H. Liu, *Chempluschem*, **2019**, DOI: 10.1002/cplu.201900568R1
- [63] D. Chen, S. Yi, W. Wu, Y. Zhong, J. Liao, C. Huang, W. Shi, *Polymer*, **2010**, 51, 3867–3878.

Entry for the Table of Contents (Please choose one layout)

FULL PAPER



Mikhail Soldatov, Hongzhi Liu*

Page No. – Page No.

POSS-phosphazene based porous material for adsorption of metal ions from water

Introduction of phosphazene units into chemical structure of POSS based porous material provides an outstanding adsorption performance for heavy metal ions. Such adsorption is caused by a coordination of the ions with nitrogen atoms of phosphazene rings.